JOURNAL OF GUIDANCE, CONTROL, AND DYNAMICS
Vol. 31, No. 5, September–October 2008

Two-Sun-Cones Attitude-Determination Method

Jozef C. van der Ha*
Kyushu University, Fukuoka 819-0395, Japan

DOI: 10.2514/1.35056

Spin stabilization offers a straightforward concept for spacecraft attitude stabilization. In the case of Earth-orbiting satellites, the determination of the spin-axis pointing direction is usually accomplished by using sun and Earth sensor measurements. For deep-space missions, however, useful Earth sensor measurements are not available. This paper presents a technique for the spin-axis attitude determination using only sun sensor data collected at two different instants of time. The spin-axis attitude corresponds to one of the intersections of the two available sun angle cones. The application of the method is validated with the help of actual in-flight sun sensor measurements from the comet nucleus tour satellite. The results indicate that the achievable attitude-determination accuracy is of the order of a degree after a number of hours. After less than two days, the error is below a tenth of a degree.

I. Introduction

THIS paper presents a revised and extended version of the conference article with the same title [1].

Spin stabilization offers a straightforward, cost-effective, and extremely robust concept for attitude stabilization. Sun sensors provide the most common measurements to be used for the attitude determination of spinning spacecraft. In the case of Earth-orbiting satellites, the sun sensor data may be merged with Earth sensor measurements [2] in order to have two independent reference directions for the attitude-determination algorithm. The spin mode is also attractive during the long cruise phases of autonomous deep-space missions because it is a low-cost design option and no further backup or safe attitude modes are required [3,4]. However, valid Earth sensor data are not available in these applications because of the large distances involved. Also, commonly available star mappers cannot be used because of the relatively high rotation rates. The approach presented here uses only sun sensor measurements (without any additional sensor data) and offers an attractive low-cost design concept for spinning deep-space probes.

The two-sun-cones (TSC) method represents a practical technique for the attitude determination of spinning satellites based on the use of *only* sun sensor measurements. The calculations may be performed on-ground or also onboard if an autonomous attitude-determination procedure is preferred. The principle of the TSC method is based on the use of two solar aspect angles ϑ_1 and ϑ_2 produced by the sun sensor at two different instants of time t_1 and t_2 (Fig. 1). The separation interval between t_1 and t_2 may be as short as a few hours but should preferably be at least a day to achieve good attitude-determination errors. The spin-axis attitude follows from the intersections of the two sun angle cones centered on the two sun vectors $\mathbf{S}_1$ and $\mathbf{S}_2$ at the times t_1 and t_2. A priori knowledge of the spacecraft pointing orientation is needed to resolve the twofold ambiguity of the attitude solution.

The achievable accuracy of the attitude estimate depends on the noise characteristics of the sun sensor, on the duration of the interval under consideration, and on the stability of the attitude pointing and of the measurement biases during the selected interval. Typical errors that can be achieved in practice are at the level of a tenth of a degree after a separation interval of one to two days. This is demonstrated with the help of actual in-flight sun sensor measurements [2] produced by the comet nucleus tour (CONTOUR) satellite.

An essential restriction for the application of the TSC method is the fact that the attitude orientation at the times t_1 and t_2 is assumed to be identical. Therefore, the results produced by the TSC method may be severely degraded if the spin-axis pointing orientation is changed or is drifting in space during the separation interval between t_1 and t_2. Fortunately, the stability condition is normally satisfied for free-drifting deep-space probes with reasonable spin rates (typically, 5 rpm or more). Solar radiation effects are the dominant disturbances affecting the pointing attitude. It is known [5] that the spin-axis pointing orientation drifts by not more than a few degrees per year for a typical deep-space satellite such as CONTOUR.

Nutation effects may introduce systematic errors in the sun aspect angle measurements, but they may effectively be eliminated by using the respective average values of the sun angles $\langle\vartheta_1\rangle$ and $\langle\vartheta_2\rangle$ collected over intervals (centered on the times t_1 and t_2) that are much longer than the nutation period. The TSC method should of course not be used if an attitude maneuver is performed during the selected interval of consideration. The same is true for an orbit maneuver unless its effect on the spin-axis attitude may be considered negligible. Also, measurement biases and other systematic modeling errors may produce significant errors in the TSC solution.

Similar techniques have been used in other missions. We located one account [6] describing the application of the sun-only attitude-determination technique for the Polar satellite, using a series of six half-hour-long data sets spanning a full day. In the cases in which sun angle measurements were taken from three data intervals, accuracies would typically be within a half-degree from the best available attitude estimate [6].

It may be mentioned that the analysis presented in this paper can readily be generalized for applications other than the one addressed here. Instead of the two close sun vector measurements, measurements from any two arbitrary close reference vectors could be used. The adopted reference vectors may even originate from two physically different sources, for instance, a star position and a magnetic field vector.

II. Geometrical Background

A. Sun Position Vectors

Figures 1 and 2 illustrate the relevant geometry and reference frames used in the formulation of the TSC attitude-determination method. The (X, Y, Z) triad represents the inertial geocentric reference frame. The sun direction within this inertial frame at the time t_1 is designated by the unit vector $\mathbf{S}_1 = \mathbf{S}(t_1)$. Similarly, the direction of the sun at a slightly later time t_2 is expressed as $\mathbf{S}_2 = \mathbf{S}(t_2)$. In general, these two unit vectors can be calculated with excellent accuracy by an analytical sun-ephemeris algorithm as given, for instance, by Vallado [7]. An approximate analytical

Presented as Paper 106 at the 17th AAS/AIAA Space Flight Mechanics Meeting, Sedona, AZ, 28 January–1 February 2007; received 9 October 2007; revision received 8 December 2007; accepted for publication 8 December 2007.

*Professor, Department of Aeronautics and Astronautics; jvdha@aol.com. Senior Member AIAA.

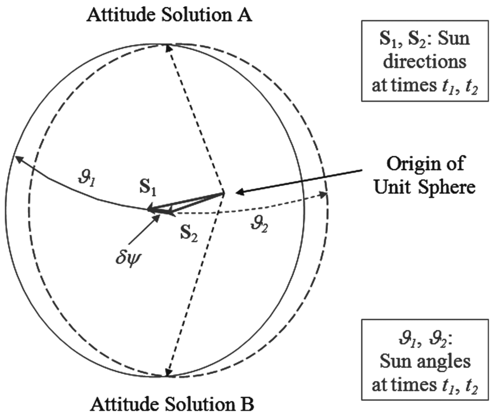

Fig. 1 Geometry of the two-sun-cones method.

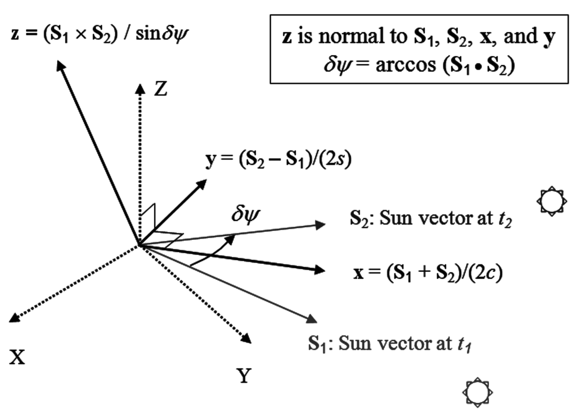

Fig. 2 Visualization of inertial (X, Y, Z) and local (x, y, z) frames.

ephemeris model with acceptable accuracy for most practical applications is presented in a previous paper [5]. This straightforward model is convenient for the visualization and interpretation of the sun vector motion over time.

The angle $\delta\psi$ denotes the arc-length separation angle between the sun vectors $\mathbf{S}_1$ and $\mathbf{S}_2$:

$$\delta\psi = \arccos(\mathbf{S}_1 \cdot \mathbf{S}_2) \tag{1}$$

When considering an interval between the two sun vectors of one day, it follows from the known sun motion in inertial space that the corresponding separation angle $\delta\psi$ amounts to almost 1 deg. In practical applications of the TSC method, intervals as small as a few hours may be selected, and so the angle $\delta\psi$ could be as small as $\delta\psi \approx 0.1$ deg.

B. Transformation of Reference Frames

Figure 2 shows the two sun vectors within the inertial (X, Y, Z) reference frame as well as in the "local" (x, y, z) frame whose axes are determined by the sun unit vectors $\mathbf{S}_1$ and $\mathbf{S}_2$. The reference axes are defined by the orthogonal unit vectors $\mathbf{x}$, $\mathbf{y}$, and $\mathbf{z}$ as follows:

$$\mathbf{x} = \tfrac{1}{2}\,(\mathbf{S}_1 + \mathbf{S}_2)/c; \qquad \mathbf{y} = \tfrac{1}{2}\,(\mathbf{S}_2 - \mathbf{S}_1)/s \\ \mathbf{z} = (\mathbf{S}_1 \times \mathbf{S}_2)/|\mathbf{S}_1 \times \mathbf{S}_2| \tag{2}$$

It can easily be shown that $|\mathbf{S}_1 \times \mathbf{S}_2| = \sin\delta\psi$. The parameters c and s in Eqs. (2) are functions of the separation angle $\delta\psi$:

$$c = \cos(\delta\psi/2); \qquad s = \sin(\delta\psi/2) \tag{3}$$

It was previously mentioned that the inertial coordinates of the two sun vectors $\mathbf{S}_1$ and $\mathbf{S}_2$ are known from ephemeris knowledge. Because of the definitions in Eqs. (2), the orientation of the local (x, y, z) frame in inertial space is known as well and can be expressed in the inertial axes (X, Y, Z) by means of the transformation matrix

$$\begin{pmatrix} x \\ y \\ z \end{pmatrix} = [T]\begin{pmatrix} X \\ Y \\ Z \end{pmatrix}$$

with

$$[T] = \frac{1}{\sin\delta\psi}\begin{bmatrix} s(S_{21} + S_{11}) & s(S_{22} + S_{12}) & s(S_{23} + S_{13}) \\ c(S_{21} - S_{11}) & c(S_{22} - S_{12}) & c(S_{23} - S_{13}) \\ (\mathbf{S}_1 \times \mathbf{S}_2)_1 & (\mathbf{S}_1 \times \mathbf{S}_2)_2 & (\mathbf{S}_1 \times \mathbf{S}_2)_3 \end{bmatrix} \tag{4}$$

The notation adopted here is such that S_{ij} (with $i = 1, 2$ and $j = 1, 2, 3$) stands for the jth inertial component of the sun unit vector $\mathbf{S}_i = \mathbf{S}(t_i)$. It is evident that the second and third rows of the matrix $[T]$ exhibit singularities in the limit when $\delta\psi \to 0$. In this case, the two sun vectors and their associated sun cones coincide, and so the component of the attitude vector that is normal to the x axis would be ill defined and a unique attitude solution cannot be established. It can be confirmed that the matrix in Eq. (4) is orthogonal (as long as $\delta\psi \neq 0$), and so its inverse equals its transpose matrix $[T]^{-1} = [T]^{\mathrm{T}}$. The matrix $[T]$ is instrumental in transforming the spin-axis attitude, which will first be determined in terms of its components along the local (x, y, z) axes, into its corresponding inertial components.

III. Construction of Attitude Solution

A. Observation Vector

The mathematics describing the TSC algorithm is similar to the well-known geometric method that employs the intersection of the sun and Earth cones derived from sun and Earth sensor measurements [8,9]. The principal difference is that the reference vectors are now provided by the two sun vectors (Figs. 1 and 2) instead of one sun vector and one Earth vector.

The fundamental measurements are the angles ϑ_1 and ϑ_2, which represent the sun aspect angles of the spin-axis attitude vector relative to the sun vectors $\mathbf{S}_1$ and $\mathbf{S}_2$, respectively. When denoting the (constant) attitude vector by z, we can formulate the two measurement equations

$$y_j = \cos\vartheta_j = (\mathbf{z} \cdot \mathbf{S}_j) \qquad j = 1, 2 \tag{5}$$

The vector $\boldsymbol{\eta} = (y_1, y_2)^{\mathrm{T}}$ is defined by the measurement angles ϑ_1 and ϑ_2 and is referred to as the "observation" vector. Equations (5) are valid regardless of the selected reference frame provided that both the attitude and the sun vectors are referred to the same frame. For the objective at hand here, it is most efficient to consider the attitude vector $\mathbf{z}$ in the local (x, y, z) frame with components written as $\mathbf{z} = (z_1, z_2, z_3)^{\mathrm{T}}$. The inertial components of the attitude vector, on the other hand, will be expressed as $\mathbf{Z} = (Z_1, Z_2, Z_3)^{\mathrm{T}}$. The transformations between the two representations of the attitude vector follow immediately from Eq. (4) as $\mathbf{z} = [T]\,\mathbf{Z}$ and $\mathbf{Z} = [T]^{\mathrm{T}}\mathbf{z}$.

B. Exact Attitude Solution

The attitude-determination algorithm within the local reference frame will now be described. First, the sun vectors $\mathbf{S}_1$ and $\mathbf{S}_2$ are written in terms of their components along the local unit vectors $\mathbf{x}$, $\mathbf{y}$, and $\mathbf{z}$ with the help of Eqs. (2), see Fig. 2:

$$\mathbf{S}_1 = c\mathbf{x} - s\mathbf{y}; \qquad \mathbf{S}_2 = c\mathbf{x} + s\mathbf{y} \tag{6}$$

When substituting these expressions into Eqs. (5), we obtain the compact observation equation

$$\boldsymbol{\eta} = [A]\boldsymbol{\zeta} \quad \text{with} \quad [A] = \begin{bmatrix} c & -s \\ c & s \end{bmatrix} \quad \text{and} \quad \boldsymbol{\zeta} = \begin{pmatrix} z_1 \\ z_2 \end{pmatrix} \tag{7}$$

This system consists of two equations and two unknowns and has the solution

$$\boldsymbol{\zeta} = [A]^{-1}\boldsymbol{\eta} \quad \text{with} \quad [A]^{-1} = \frac{1}{\sin\delta\psi}\begin{bmatrix} s & s \\ -c & c \end{bmatrix} \tag{8}$$

The singularity for $\delta\psi \to 0$ has been previously addressed and resurfaces in Eq. (8) because $\det[A] = \sin\delta\psi$. Therefore, the solution $\boldsymbol{\zeta} = [A]^{-1}\boldsymbol{\eta}$ becomes ill defined when $\delta\psi \to 0$.

The result of Eq. (8) may be written explicitly in terms of the measured sun aspect angles

$$z_1 = \tfrac{1}{2}(\cos\vartheta_2 + \cos\vartheta_1)/c; \qquad z_2 = \tfrac{1}{2}(\cos\vartheta_2 - \cos\vartheta_1)/s \tag{9}$$

The attitude solution of Eq. (9) is exact in the sense that no approximations have been made in the derivation. Of course, the resulting attitude solution is normally contaminated by random errors as well as by unknown biases in the sun angle measurements. It may be noted that by virtue of the unit-vector constraint

$$z_3 = \pm\sqrt{1 - z_1^2 - z_2^2}$$

the knowledge of

$$\boldsymbol{\zeta} = (z_1, z_2)^{\mathrm{T}}$$

produces the complete attitude vector (apart from the sign ambiguity). The component z_1 remains well defined for $\delta\psi \to 0$ as expected, whereas both z_2 and z_3 apparently suffer severe singularities in that case.

C. Asymptotic Attitude Solution

To gain insight into the nature of the singularity of the attitude solution, we look for an asymptotic approximate solution with validity for $\delta\psi \to 0$. First, we introduce the mean value ϑ of the two sun aspect angles and the difference $\delta\vartheta$ between these angles:

$$\vartheta = (\vartheta_2 + \vartheta_1)/2; \qquad \delta\vartheta = \vartheta_2 - \vartheta_1 \tag{10}$$

The results of Eqs. (9) can now be expressed as

$$z_1 = F(\delta\vartheta, \delta\psi)\cos\vartheta; \qquad z_2 = -G(\delta\vartheta, \delta\psi)\sin\vartheta \tag{11}$$

with

$$\begin{aligned} F(\delta\vartheta, \delta\psi) &= \cos(\delta\vartheta/2)/\cos(\delta\psi/2); \\ G(\delta\vartheta, \delta\psi) &= \sin(\delta\vartheta/2)/\sin(\delta\psi/2) \end{aligned} \tag{12}$$

It is important to recognize that the difference in the sun aspect angles $\delta\vartheta$ can never be larger than the motion of the sun vector itself during the separation interval, $|\delta\vartheta| < |\delta\psi|$, under the assumption that the attitude remains fixed in space. Because both $\delta\psi$ and $\delta\vartheta$ are small angles of a few degrees at most, it can be seen that the function $F \approx 1$ and, furthermore, $F > 1$. The function $G \approx \delta\vartheta/\delta\psi$ can be shown to lie within the interval $[-1, 1]$ and remains well defined for $\delta\psi \to 0$.

Asymptotic expansions of the functions F and G can easily be established:

$$F(\delta\vartheta, \delta\psi) \approx 1 + \{(\delta\psi)^2 - (\delta\vartheta)^2\}/8 + O\{(\delta\psi)^4\} \tag{13a}$$

$$G(\delta\vartheta, \delta\psi) \approx (\delta\vartheta/\delta\psi)\left[1 + \{(\delta\psi)^2 - (\delta\vartheta)^2\}/24 + O\{(\delta\psi)^4\}\right] \tag{13b}$$

The expression $O\{(\delta\psi)^4\}$ represents terms of fourth-order smallness, for instance, $(\delta\psi)^4$, $(\delta\vartheta)^4$, and $(\delta\psi)^2(\delta\vartheta)^2$.

When considering intervals of up to five days, the angular contributions of the quadratic terms in Eqs. (13) are typically well below 0.05 deg. Therefore, the following first-order approximate results may be sufficiently accurate in practice:

$$z_1 \approx \cos\vartheta + O\{(\delta\psi)^2\}; \qquad z_2 \approx -(\delta\vartheta/\delta\psi)\sin\vartheta + O\{(\delta\psi)^2\} \tag{14}$$

This confirms that the component z_2 may be affected by the singularity for $\delta\psi \to 0$, whereas z_1 is not. This can be understood because z_1 is calculated from the two (equal) sun aspect angles and remains well defined when the two sun cones coincide. The component z_2, on the other hand, follows from the intersections of the two sun cones and becomes ill defined when $\delta\psi \to 0$.

D. Attitude Component z_3

The third attitude component z_3 cannot be determined independently from the measurement equations in Eq. (7) due to the definition of the local frame using the two sun vectors. The component z_3 can be expressed in z_1 and z_2 by employing the unit-vector constraint $|z| = 1$:

$$z_3 = \pm\sqrt{1 - z_1^2 - z_2^2} = \pm\sqrt{1 - (\boldsymbol{\zeta}\cdot\boldsymbol{\zeta})} \tag{15}$$

The sign of z_3 must be resolved from a priori attitude knowledge. The product $(\boldsymbol{\zeta}\cdot\boldsymbol{\zeta})$ can be expressed in the components of the observation vector $\mathbf{y}$ with the help of Eq. (8):

$$(\boldsymbol{\zeta}\cdot\boldsymbol{\zeta}) = \boldsymbol{\eta}^{\mathrm{T}}[A^{-1}]^{\mathrm{T}}[A^{-1}]\boldsymbol{\eta} = \{y_1^2 + y_2^2 - 2y_1y_2\cos\delta\psi\}/\sin^2\delta\psi \tag{16}$$

Alternatively, we may use the results of Eqs. (11) and (12). Either way we obtain

$$(\boldsymbol{\zeta}\cdot\boldsymbol{\zeta}) = z_1^2 + z_2^2 = F^2\cos^2\vartheta + G^2\sin\vartheta \tag{17}$$

When using the asymptotic results of Eqs. (13), the following expression for z_3^2 is found:

$$\begin{aligned} z_3^2 \approx{}& \{1 - (\delta\vartheta/\delta\psi)^2\}\left[\sin^2\vartheta - (\delta\psi)^2\{3\cos^2\vartheta\right. \\ &\left. + (\delta\vartheta/\delta\psi)^2\sin^2\vartheta\}/12\right] + O\{(\delta\psi)^4\} \end{aligned} \tag{18}$$

Thus, the leading-term asymptotic result for the component z_3 is

$$z_3 \approx \pm\sqrt{\{1 - (\delta\vartheta/\delta\psi)^2\}}\sin\vartheta + O\{(\delta\psi)^2\} \tag{19}$$

Equations (14) and (19) confirm that the leading terms of the attitude components indeed make a unit vector (within the adopted approximations). In fact, the same property can also be shown to hold if the neglected smaller second-order terms are included.

E. Special Cases for Attitude Vector

An interesting special case occurs when $\delta\vartheta \approx \pm\delta\psi$. In this case, we find $z_3 \approx 0$ from Eq. (19) with errors of second-order smallness. It can be seen that the attitude vector $\mathbf{z}$ lies within the plane formed by the two sun vectors (i.e., the ecliptic plane). Equations (14) show that $z_1 \approx \cos\vartheta$ and $z_2 \approx \pm\sin\vartheta$ with errors of second-order smallness.

Another special case occurs when $\delta\vartheta \approx 0$, and so the leading terms of the attitude solution are $z_1 \approx \cos\vartheta$, $z_2 \approx 0$, and $z_3 \approx \pm\sin\vartheta$. In this case, the attitude vector lies within the (x, z) plane normal to the ecliptic. When, in addition, ϑ equals 90 deg, the attitude is oriented normal to the ecliptic plane. Finally, in the special case in which $\vartheta \approx 0$, we find $z_1 \approx 1$ and $z_2 \approx z_3 \approx 0$, and the attitude vector $\mathbf{z}$ lies midway between the two sun vectors.

IV. Error Covariance Results

A. Covariance of $\boldsymbol{\zeta}$

It is of interest to calculate the covariances of the approximate attitude solution on the basis of the specified sun sensor random-noise errors. In particular, it is important to understand how the separation angle $\delta\psi$ affects the achievable precision of the attitude knowledge in view of the singularity for $\delta\psi \to 0$.

The measurements ϑ_1 and ϑ_2 are taken at different times that are sufficiently far apart to eliminate any potential autocorrelation of the sensor random noise. Therefore, it is justifiable to assume that their noise terms are not correlated, that is, $E\{(\Delta\vartheta_1)(\Delta\vartheta_2)\} = 0$. Furthermore, the variance of the random noise at the two instants t_1 and t_2 can be considered equal, that is, $E\{(\vartheta_1)^2\} = E\{(\Delta\vartheta_2)^2\} = \sigma_\vartheta^2$. Therefore, the error covariance matrix $[C(\boldsymbol{\eta})]$ of the observation vector $\boldsymbol{\eta}$ can be written as [see Eqs. (5) and (7)]

$$[C(\boldsymbol{\eta})] = E\{[\Delta\boldsymbol{\eta}\Delta\boldsymbol{\eta}^{\mathrm{T}}]\} = \sigma_\vartheta^2 \begin{bmatrix} \sin^2\vartheta_1 & 0 \\ 0 & \sin^2\vartheta_2 \end{bmatrix}$$
$$\approx \sigma_\vartheta^2 \sin^2\vartheta \begin{bmatrix} 1 - \delta\vartheta/\tan\vartheta & 0 \\ 0 & 1 + \delta\vartheta/\tan\vartheta \end{bmatrix} + O\{(\delta\vartheta)^2\} \quad (20)$$

The covariance matrix of the attitude solution follows now from Eqs. (8) and (20)

$$[C(\boldsymbol{\zeta})] = \begin{bmatrix} E\{(\Delta z_1)^2\} & E\{(\Delta z_1)(\Delta z_2)\} \\ E\{(\Delta z_1)(\Delta z_2)\} & E\{(\Delta z_2)^2\} \end{bmatrix} = E\{[\Delta\boldsymbol{\zeta}\Delta\boldsymbol{\zeta}^{\mathrm{T}}]\}$$
$$= [A]^{-1}[C(\boldsymbol{\eta})][A^{-1}]^{\mathrm{T}} \approx \tfrac{1}{2}\sigma_\vartheta^2 \sin^2\vartheta \begin{bmatrix} 1/c^2 & \delta\vartheta/(sc\tan\vartheta) \\ \delta\vartheta/(sc\tan\vartheta) & 1/s^2 \end{bmatrix} \quad (21)$$

When expanding for small $\delta\psi$ and neglecting terms of order $(\delta\psi)^2$ and higher, the diagonal terms in the matrix in Eq. (21) take the form

$$\sigma_1^2 = E\{(\Delta z_1)^2\} \approx \tfrac{1}{2}\sigma_\vartheta^2 \sin^2\vartheta \rightarrow \sigma_1 \approx \tfrac{1}{2}\sqrt{2}\,\{\sigma_\vartheta \sin\vartheta\} \quad (22a)$$

$$\sigma_2^2 = E\{(\Delta z_2)^2\} \approx 2\sigma_\vartheta^2 \sin^2\vartheta/(\delta\psi)^2 \rightarrow \sigma_2 \approx \sqrt{2}\,\{\sigma_\vartheta \sin\vartheta\}/\delta\psi \quad (22b)$$

This result represents a very elongated error parallelogram with the long diagonal along the z_2 axis (see Wertz [8], Sec. 10.1).

B. Interpretation of Covariances of $\boldsymbol{\zeta}$

The matrix in Eq. (21) shows that the error covariances σ_1 and σ_2 of the attitude components z_1 and z_2 are correlated through the off-diagonal covariance terms, denoted as σ_{12}, which depend on the angle $\delta\vartheta$. The associated correlation coefficient ρ_{12} follows from Eqs. (21), (22a), and (22b):

$$\sigma_{12} \approx (\delta\vartheta/\delta\psi)\sigma_\vartheta^2 \sin\vartheta\cos\vartheta \rightarrow \rho_{12} = \sigma_{12}/(\sigma_1\sigma_2) \approx \delta\vartheta/\tan\vartheta \quad (23)$$

This result indicates that the correlation between the errors of the two attitude components z_1 and z_2 is relatively weak (as long as the sun aspect angle $\vartheta \gg \delta\vartheta$). For example, when considering a separation interval of five days at most and a sun aspect angle in the interval $60 < \vartheta < 120$ deg, we obtain $\rho_{12} < 0.05$.

The result in Eq. (22a) implies that the expected error σ_1 in the attitude component z_1 is in any case smaller than the magnitude of the input random noise of the sun aspect angle σ_ϑ due to the beneficial effect of having two independent sun angle measurements. On the other hand, the expected error σ_2 in Eq. (22b) is significantly degraded by the singularity for $\delta\psi \rightarrow 0$. It is important, however, to recognize that σ_2 decreases when increasing the separation angle $\delta\psi$ between the two sun positions $\mathbf{S}_1$ and $\mathbf{S}_2$. In fact, the error σ_2 can be made arbitrarily small by choosing a sufficiently large separation angle (i.e., $\delta\psi \gg \sigma_\vartheta$). If we require $\sigma_2 < \varepsilon$ with ε denoting a specified error threshold, Eq. (22b) produces the useful condition

$$\delta\psi > \sqrt{2}\,\{\sigma_\vartheta \sin\vartheta\}/\varepsilon \quad (24)$$

Figure 3 provides an illustration of the implications of this result for the special case $\vartheta \approx 90$ deg, that is, for an attitude normal to the ecliptic plane. It provides the length of the separation interval in days that is required in order that the variance of the z_2 attitude component reaches a certain specified error threshold for a range of sun sensor random-noise specifications. The selected thresholds cover the range from 0.1 to 0.5 deg. The root-mean-square (rms) value of the random noise of the sun aspect angle measurements is of the order of $\sigma_\vartheta = 10^{-3}$ deg for sun sensors used in demanding mission applications [2]. The range of sun aspect angle noise from 0.001 to 0.01 deg in Fig. 3 incorporates essentially all existing sun sensors for spinning satellites.

For illustration, if we take a sensor random noise of $\sigma_\vartheta = 0.005$ deg and require an error threshold of $\varepsilon = 0.1$ deg, Fig. 3 predicts that the required separation interval would be four days (when assuming a sun angle $\vartheta \approx 90$ deg). Of course, the attitude is expected to remain constant throughout the interval under consideration.

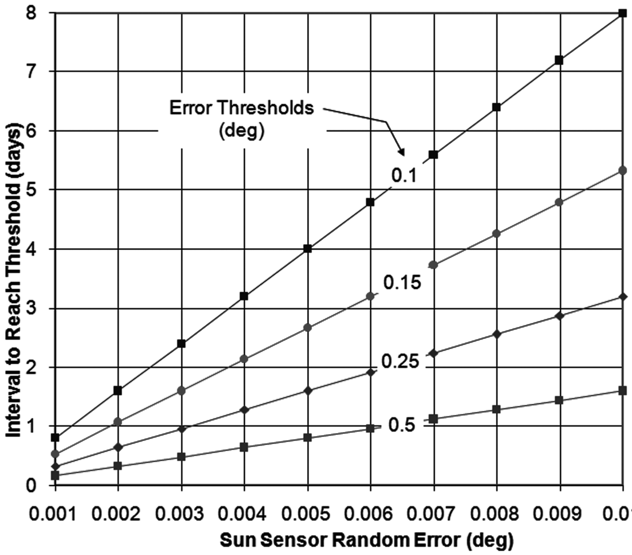

Fig. 3 Required interval to achieve specified error thresholds for z_2 ($\vartheta \approx 90$ deg).

C. Covariances of z_3 Component

The error covariances of the third attitude component z_3 can be calculated with the help of the normality condition in Eq. (15):

$$\sigma_3^2 = E\{(\Delta z_3)^2\} = E\{(\Delta z_3^2)^2\}/(4z_3^2) = E\{[\Delta(\boldsymbol{\zeta}^{\mathrm{T}}\boldsymbol{\zeta})]^2\}/(4z_3^2)$$
$$= \boldsymbol{\zeta}^{\mathrm{T}}[C(\boldsymbol{\zeta})]\boldsymbol{\zeta}/z_3^2 = 2\sigma_\vartheta^2 \sin^2\vartheta\{s^2 z_1^2 + c^2 z_2^2$$
$$+ 2scz_1z_2\delta\vartheta/\tan\vartheta\}/(z_3 \sin\delta\psi)^2 \quad (25)$$

This result is exact and may be expanded asymptotically in accordance with the different orders of magnitude of the contributing terms:

$$\sigma_3^2 \approx 2\sigma_\vartheta^2 \frac{\sin^2\vartheta}{z_3^2}\left\{\frac{z_2^2}{(\delta\psi)^2} + \frac{z_1z_2}{\tan\vartheta}\left(\frac{\delta\vartheta}{\delta\psi}\right) + \frac{z_1^2}{4}\right\} \quad (26)$$

The term containing $1/(\delta\psi)^2$ dominates the other terms for small $\delta\psi$, and so we have

$$\sigma_3 \approx \sqrt{2}\,\sigma_\vartheta \sin\vartheta|z_2/z_3|/\delta\psi \quad (27)$$

This result exhibits another singularity (in addition to the one for $\delta\psi \rightarrow 0$) appearing in the limit for $z_3 \rightarrow 0$. When substituting the results for z_2 and z_3 of Eqs. (14) and (19) into Eq. (27), we find

$$\sigma_3 \approx \sqrt{2}\,\sigma_\vartheta \sin\vartheta\,(\delta\vartheta/\delta\psi)/\sqrt{(\delta\psi)^2 - (\delta\vartheta)^2} \quad (28)$$

This expression confirms that the singularity $z_3 \rightarrow 0$ is equivalent to $|\delta\vartheta/\delta\psi| \rightarrow 1$, as is evident from Eq. (19). In this case, the spin-axis attitude lies in the (ecliptic) plane formed by the two sun vectors. Therefore, the two sun cones do not intersect but are tangent to each other (see Fig. 4) and the error in the component z_3 is extremely sensitive to errors in the sun angle measurements, which leads to the large value of the covariance term σ_3.

The off-diagonal covariance term σ_{13} can now be calculated as follows:

$$\sigma_{13} = E\{(\Delta z_1\Delta z_3)\} = -E\{(\Delta z_1)(z_1\Delta z_1 + z_2\Delta z_2)\}/z_3 = -(z_1\sigma_1^2$$
$$+ z_2\sigma_{12})/z_3 \approx -\tfrac{1}{2}\sigma_\vartheta^2 \sin^2\vartheta\{z_1 + 2z_2(\delta\vartheta/\delta\psi)/\tan\vartheta\}/z_3 \quad (29)$$

This expression suffers from the singularity for $z_3 \rightarrow 0$ or $|\delta\vartheta/\delta\psi| \rightarrow 1$ as discussed following Eq. (28). The correlation coefficient ρ_{13} can be calculated as

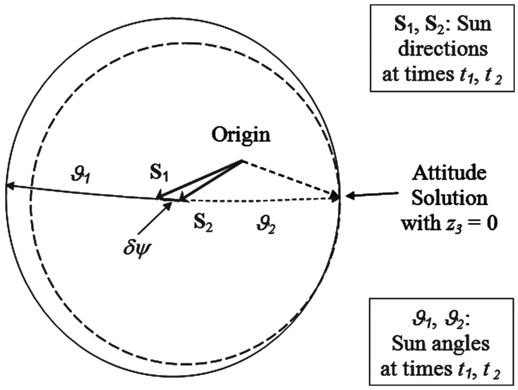

Fig. 4 Illustration of coplanarity of attitude and sun vectors ($\delta\vartheta = -\delta\psi$).

$$\rho_{13} = \sigma_{13}/(\sigma_1\sigma_3) \approx -\tfrac{1}{2}\{z_1\delta\psi/z_2 + 2\delta\vartheta/\tan\vartheta\} \approx O(\delta\psi) \quad (30)$$

This result indicates that the components z_1 and z_3 are weakly correlated, as are z_1 and z_2.

The off-diagonal covariance term σ_{23} follows similarly as σ_{13} in Eq. (29):

$$\sigma_{23} = E\{(\Delta z_2\Delta z_3)\} = -(z_1\sigma_{12} + z_2\sigma_2^2)/z_3$$
$$\approx -\sigma_\vartheta^2 \sin^2\vartheta\,\{2z_2/(\delta\psi)^2 + z_1(\delta\vartheta/\delta\psi)/\tan\vartheta\}/z_3 \quad (31)$$

The asymptotic result for $\delta\psi \to 0$ is produced by the first term in parentheses:

$$\sigma_{23} \approx -2\sigma_\vartheta^2 \sin^2\vartheta\,(z_2/z_3)/(\delta\psi)^2 \quad (32)$$

The correlation coefficient ρ_{23} follows as

$$\rho_{23} = \sigma_{23}/(\sigma_2\sigma_3) \approx -1 \quad (33)$$

This result indicates that the components z_2 and z_3 are strongly correlated, which is a consequence of the way the z_3 component is established, namely, by means of the normality condition in Eq. (15). Thus, the z_2 and the z_3 components suffer more or less equally from the fact that the two sun angle measurements essentially provide information on the attitude component z_1 only.

D. Attitude Error

The expected angular error in the spin-axis pointing direction is represented by the sum of the covariances:

$$\sigma_{\text{att}}^2 = \sigma_1^2 + \sigma_2^2 + \sigma_3^2 \approx \tfrac{1}{2}\sigma_\vartheta^2 \sin^2\vartheta\{1 + 4/(\delta\psi)^2 + 4z_2^2/(z_3\delta\psi)^2\} \quad (34)$$

When performing the asymptotic expansion for $\delta\psi \to 0$, we find the leading term

$$\sigma_{\text{att}}^2 \approx 2\sigma_\vartheta^2 \sin^2\vartheta\{1 + z_2^2/z_3^2\}/(\delta\psi)^2 \approx 2\sigma_\vartheta^2 \sin^2\vartheta/\{(\delta\psi)^2 - (\delta\vartheta)^2\} \quad (35)$$

This result confirms that the attitude error lies essentially in the (y, z) plane because the z_1 component is known accurately from the sun sensor measurements. Equation (35) contains the singularity for the case $|\delta\vartheta/\delta\psi| \to 1$, in which the attitude error becomes large. In this case, the two sun cones do not intersect but are tangent, as addressed previously and illustrated in Fig. 4.

An interesting situation occurs in the case $\delta\vartheta \approx 0$, which implies that $z_1 \approx \cos\vartheta$, $z_2 \approx 0$, and $z_3 \approx \pm\sin\vartheta$, and so the attitude vector lies close to the (x, z) plane bisecting the two sun vectors. In this case, the result for the attitude covariance becomes

$$\sigma_{\text{att}}^2 \approx 2\sigma_\vartheta^2 \sin^2\vartheta/(\delta\psi)^2 < 2\sigma_\vartheta^2/(\delta\psi)^2 \quad (36)$$

The upper limit is reached when $\vartheta = 90$ deg, that is, when the attitude is pointing normal to the ecliptic plane. It may be noted that the result in Eq. (36) is identical to the expression for σ_2^2 in Eq. (22b) and illustrated in Fig. 3. Thus, the results shown in Fig. 3 are also relevant for the attitude error, at least in the particular case in which $\delta\vartheta \approx 0$ and $\vartheta = 90$ deg, as considered here. The reason is that the error in z_1 is negligible and the attitude is a unit vector pointing in the z_3 direction (when $\vartheta = 90$ deg), and so the error must be along the z_2 direction.

V. Measurement Errors

A. Processing Measurements

The application of the TSC method uses two sun aspect angles taken at two instants of times t_1 and t_2, which may be separated by a period of a few hours up to a number of days. Thus, two sets of sun angle measurements $\vartheta_k^{(j)}$ with $j = 1, \ldots, m$ are collected over the two intervals $k = 1, 2$. These data are averaged to obtain the effective sun angle measurements ϑ_1 and ϑ_2 at the averaged centers t_1 and t_2 of the selected intervals

$$\vartheta_k = \vartheta(t_k) = \frac{1}{m}\sum_{j=1,\ldots,m}\{\vartheta(t_k^{(j)})\} \quad \text{for } k = 1, 2 \quad (37)$$

The lengths of the two data intervals should be a sufficiently large multiple of the nutation period so that effects caused by nutation on the TSC attitude solution will be filtered out. When collecting two sets of $m(\geq 100)$ data centered on the times t_1 and t_2, the effective measurement noise can be reduced by a factor of $\sqrt{m}\,(\geq 10)$. In that case, the effective random error in the resulting attitude solution decreases by the same factor.

B. Discussion of Biases

Figure 3 shows that the random-noise effect on the attitude error can be made arbitrarily small by selecting the appropriate separation interval between the two sun vectors. It should be kept in mind, however, that the separation interval must be sufficiently long to be able to surmount the singularity. For instance, for the random noise of 0.001 deg in Fig. 3, the separation interval must be close to a day (i.e., 19.5 h) to achieve the attitude-determination error of 0.1 deg. This raises the important issue about the potential effect of systematic errors or biases (which typically have a much larger magnitude than the random noise) on the resulting attitude-determination error. Furthermore, the biases rather than the random errors drive the achievable attitude-determination accuracy in practical applications [10]. The results of the TSC method (such as those of any attitude-determination method) should be expected to be contaminated by the effects of unknown measurement and modeling biases.

Because biases typically vary slowly with time, their effects on the sun angle measurements may be expected to be largely identical during each of the two data intervals selected in the application of the TSC method. Therefore, the effective bias (i.e., the sum of all active biases) may be broken up in an absolute part that has an identical effect on the sun angle throughout both data intervals, plus a smaller time-varying differential part that acts differently on the sun angles in the two intervals.

Although it is difficult to reach a good understanding of the actual biases that may be acting in practice, Table 1 summarizes a few of the relevant biases. The sun sensor internal bias includes effects caused by power-supply variations and thermal drifts. The other biases in Table 1 originate from spacecraft and system-level error contributions. The middle column lists the expected worst-case constant absolute values of the biases. The right-hand column provides a conjecture of the potential variations of these biases over a period of one week, which amounts to the differential bias mentioned previously.

The effects of the biases listed in Table 1 on the resulting effective sun angle measurements ϑ_1 and ϑ_2 in the two intervals are designated by δ_k ($k = 1, 2$) so the measured ϑ_k equals the unknown actual $\vartheta_{k,\text{act}}$ plus the bias error δ_k for $k = 1, 2$. Therefore, the angles ϑ and $\delta\vartheta$ defined in Eqs. (10) may be split up in terms of their actual values plus the bias effects

Table 1 Absolute and relative biases affecting sun angle measurements (worst case)

Systematic error or bias	Absolute value, deg	Variation over 1 week, deg
Dynamical imbalance	0.2	0.01
Sun sensor internal	0.1	0.02
Mounting misalignments	0.1	0.01
Sun-ephemeris errors	0.02	0.01
Other effects	0.05	0.01
Total (RSS)	≈0.25	≈0.03

$$\vartheta = \vartheta_{\text{act}} + \delta \quad \text{with} \quad \delta = \tfrac{1}{2}(\delta_1 + \delta_2) \tag{38a}$$

$$\delta\vartheta = \delta\vartheta_{\text{act}} + \delta_2 - \delta_1 \tag{38b}$$

Thus, δ designates the absolute or constant part of the bias and $\delta_2 - \delta_1$ is the differential part. The absolute bias δ induces a systematic error in the resulting TSC attitude solution in the same way as happens for any other attitude-determination method that takes account of random errors only. The differential part of the bias, on the other hand, is particularly relevant for the TSC method due to the subtraction of the effective sun angles ϑ_1 and ϑ_2 measurements in the two intervals as shown explicitly in the result for $\delta\vartheta$ in Eq. (38b). The repercussions of the differential bias on the TSC attitude solution will be studied next.

C. Effect of Differential Bias

Equations (38) show that the mean sun aspect angle measurement $\vartheta = (\vartheta_1 + \vartheta_2)/2$ is affected only by the absolute bias δ, whereas the angle $\delta\vartheta$ is influenced only by the differential bias $\delta_2 - \delta_1$. The corresponding errors in the attitude components can readily be calculated from Eqs. (14) and (19). It follows that z_1, such as ϑ, is affected only by the absolute bias δ. The components z_2 and z_3, on the other hand, are affected by the absolute bias δ as well as by the differential bias $\delta_2 - \delta_1$. When focusing on the effect of the differential bias, we find

$$\begin{aligned} |\delta z_{2,\text{diff}}| &\approx \sin\vartheta |\delta_2 - \delta_1|/\delta\psi + O\{(\delta\psi)^2\} \\ |\delta z_{3,\text{diff}}| &= (z_2/z_3)\,|\delta z_{2,\text{diff}}| \end{aligned} \tag{39}$$

For simplicity, we assume now that the spin-axis attitude is oriented away from the ecliptic plane so that $z_3 > z_2$. This condition would be satisfied, for instance, in the design of the hibernation mode of a deep-space probe, in which it makes good sense to orient the spin axis close to the normal of the ecliptic plane [3–5]. The maximum half-cone pointing attitude error induced by the differential bias may now be approximated as

$$|\delta \mathbf{z}_{\text{diff}}| \approx \sqrt{(1 + z_2^2/z_3^2)}\,|\delta z_{2,\text{diff}}| < |\sqrt{2}\,|\delta_2 - \delta_1|/\delta\psi \tag{40}$$

The sun's angular motion $\delta\psi$ during the separation interval may be approximated by $\delta\psi \approx 0.9856° \times d$ where d is expressed in days. On the basis of the worst-case differential bias of 0.03 deg after a separation interval of one week (see Table 1), Eq. (40) may be quantified as

$$|\delta \mathbf{z}_{\text{diff}}| < \sqrt{2}\,(0.03 \ \text{deg})/(0.9856 \ \text{deg} \times 7) \approx 0.35 \ \text{deg} \tag{41}$$

In many practical cases, the vector $\delta\mathbf{z}_{\text{diff}}$ is approximately normal to the vector $\mathbf{z}$, in particular when the spin-axis attitude is close to the (y, z) plane, which corresponds to sun angles of the order of 90 deg. In those cases, z_1 is small and $(\mathbf{z} \cdot \delta\mathbf{z}_{\text{diff}}) \approx 0$ follows from the unit-vector constraint. The result in Eq. (41) may thus be interpreted as the worst-case half-cone angular error in the attitude knowledge induced by the worst-case differential bias of 0.03 deg between the two effective sun angle measurements (after a one-week separation interval).

Equation (41) provides the expected attitude error at only one point in time, namely after one week. For earlier points in time, the singularity for $\delta\psi \to 0$ in Eq. (40) may lead to difficulties. To analyze the evolution of the attitude error induced by the differential bias, we assume that the evolution of $|\delta_2 - \delta_1|$ may be modeled realistically by a random-walk process (see Gelb [11]). This means that its derivative is represented by a Gaussian zero-mean white-noise random variable $n(d)$, expressed in days d, with expected value $E\{n(d)\} = 0$ and variance $E\{n^2(d)\} = \sigma_n^2$.

After integrating the random-noise $n(d)$, the variance of the differential bias σ_{diff}^2 can be expressed in terms of the power spectral density (PSD) function Φ of the white-noise $n(d)$:

$$\sigma_{\text{diff}}^2 = E\{|\delta_2 - \delta_1|^2\} = \Phi d \tag{42}$$

A practical estimate of the PSD function Φ can be established by recognizing that the differential bias reaches its predicted worst-case value of 0.03 deg after $d = 7$ days (Table 1). Thus, the variance $\sigma_{\text{diff}}(d = 7) \approx 0.01$ deg and the numerical value of the PSD follows from Eq. (42):

$$\Phi \approx \sigma_{\text{diff}}^2/d \approx (0.01 \ \text{deg})^2/7 \approx 1.43 \times 10^{-5} \ (\text{deg})^2/\text{day} \tag{43}$$

Finally, the variance of the attitude error induced by the differential bias can be established from Eqs. (40–43):

$$\begin{aligned} \sigma_{\text{att,diff}}^2 &= E\{|\delta\mathbf{z}_{\text{diff}}|^2\} < 2E\{|\delta_2 - \delta_1|^2\}/(\delta\psi)^2 = 2\Phi d/(\delta\psi)^2 \\ &\to \sigma_{\text{att,diff}} \approx \sqrt{(2\Phi d)}/(0.9856 \ \text{deg} \times d) = 5.42 \times 10^{-3}/\sqrt{d} \\ &= 0.31 \ \text{deg}/\sqrt{d} \end{aligned} \tag{44}$$

As expected, this result is consistent with the 3σ-level attitude error after one week in Eq. (41).

Figure 5 illustrates the evolution of the attitude-determination error for three differential bias levels ranging from typical to exaggerated worst case. Whereas the detrimental effect of the singularity for $\delta\psi \to 0$ is quite apparent, the error decreases continuously over time and starts leveling off after a week. The expected worst-case attitude-determination error, corresponding to the differential bias of 0.03 deg, falls below the 1 deg level within one day and is smaller than 0.5 deg after about 3.5 days.

VI. Validation Using CONTOUR Data

The application of the two-sun-cones method has been validated with the help of actual in-orbit sun sensor measurements generated by the CONTOUR spacecraft during its Earth-phasing orbits [1]. Sun sensor data are available over the four Earth sensor coverage intervals during the last four orbits (of about 41.5-h period) before the solid rocket motor (SRM) firing on 15 August 2002. The lengths of the sensor-data intervals considered for the present analysis vary from about one to three hours and cover a total period of about five days.

When considering CONTOUR's spin rate of 59.7 rpm, it is evident that the free-drift pointing motion of the spin axis should remain very limited [5], that is, well below 0.1 deg over the five-day period. However, a relatively minor attitude correction maneuver (no. 12 in Table 1, Ref. [2]) of about 0.2 deg in length was performed between the second and third sensor-coverage interval. Therefore, the most suitable data for the validation of the TSC method are provided by the two pairs of data intervals before and after the maneuver. Three separate batches of data, each containing 200 individual sensor measurements, are taken at the start, in the middle, and at the end of each of the two data intervals. Thus, nine TSC

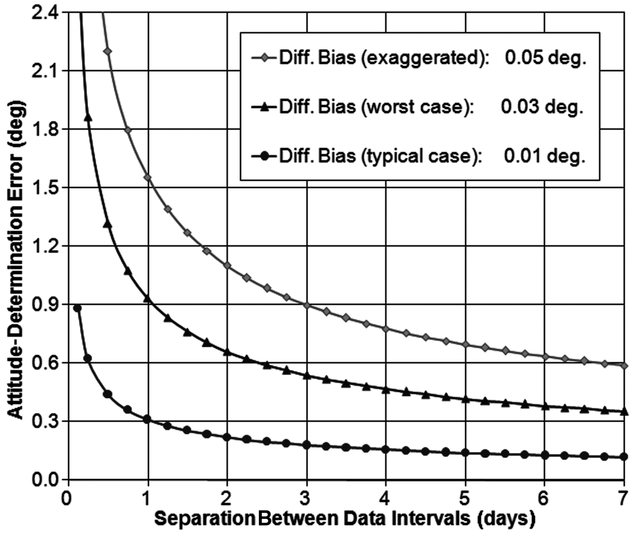

Fig. 5 Predicted attitude-determination error due to differential bias.

attitude-determination results are obtained from the two intervals before the maneuver, and another nine results are obtained when using the pair of data intervals after the maneuver. The resulting separation intervals are close to the orbit period, that is, of the order of 41.5 h with variations of ±2.5 h.

The results of these simulations are summarized in Table 2. The reference attitudes in the third column are written in terms of their right ascension and declination angles relative to the J2000 geocentric inertial frame. They represent the best available estimates of the spin-axis attitude (see Table 2 in Ref. [2]). It follows that the mean error is about 0.075 deg for the collection of 18 runs in Table 2, with separation intervals ranging from about 39 to 43 h. The results in Table 2 are consistent with the theoretical predictions in Fig. 3. After a separation interval of about 1.7 days, the attitude error should be less than 0.1 deg for a sun angle random error in the range 0.001–0.002 deg. This consistency implies that effects due to differential biases must have been small, in any case well below the typical bias levels illustrated in Fig. 5.

Table 3 summarizes the results of the TSC method over different (and generally longer) separation intervals that do contain the disturbance due to the 0.2-deg maneuver. The reference attitude for the comparison is taken midway between the best estimates before and after the maneuver. It can be seen that the errors increase with decreasing separation intervals as expected. The attitude-determination results are clearly degraded when compared with those in Table 2 and with the predictions in Fig. 3.

When comparing the magnitude of the mean errors for the different separation intervals, we observe that there is an almost perfect inversely proportional relationship between the attitude error and the separation time, that is, attitude error $\approx 2.55\ \mathrm{deg}/d$. (The correspondence is even better when the second and third rows with intervals of about 3.4 days are combined in one row.) The proportionality relationship is very different from the results for differential biases shown in Fig. 5. This is, of course, due to the fact that the magnitude of the attitude maneuver is constant and, thus, independent of the length of the separation interval, whereas the differential bias is expected to increase with the square root of time [see Eq. (44)].

Table 4 provides the results of the TSC method over very short separation intervals of about 3, 2, 1, and 0.5 h. Figure 3 predicts that the attitude-determination errors should be at least 0.5 deg (and larger for the shorter intervals) due to the effect of the singularity. Table 4 shows that the mean errors are in fact over 1 deg for the four separation intervals considered. The last two entries of the minimum errors, however, are well below 1 deg, but they do not follow the expected trend (which may partly be due to the unequal number of samples for the different cases). The maximum errors, on the other hand, increase with decreasing separation intervals as expected. The results confirm that the attitude errors of the TSC method for relatively short intervals should be expected to be over 1 deg. This is consistent with the predictions of Figs. 3 and 5. It may be noted that a small differential bias of 0.01 deg may lead to an attitude error of 0.9 deg for the 3-h separation interval (see Fig. 5) and an even larger error for the shorter intervals.

VII. Conclusions

The two-sun-cones attitude-determination method produces a complete spin-axis attitude solution using sun sensor measurements only. The methodology and operations principle of the TSC technique are presented and evaluated in detail. Practically useful asymptotic expressions for the attitude solution are established. Actual flight data of the CONTOUR satellite are used to illustrate and validate the method. It is shown that, for a separation interval of less than two days, the mean error from a total of 18 runs is well below a tenth of a degree and the maximum error is only slightly above that

Table 2 Validation of TSC method using CONTOUR data (over intervals of 39 to 44 h)

Data	Runs	Reference attitude, deg	Minimum error, deg	Mean error, deg	Maximum error, deg	Standard deviation, deg
1 & 2	9	(258.44, 28.96)	0.044	**0.083**	0.136	**0.037**
3 & 4	9	(258.61, 29.15)	0.053	**0.068**	0.094	**0.015**

Table 3 TSC results using CONTOUR data (over maneuver)

Data	Runs	Separation interval, days	Minimum error, deg	Mean error, deg	Maximum error, deg	Standard deviation, deg
1 & 4	9	5.16 ± 0.04	0.480	**0.498**	0.532	**0.024**
1 & 3	9	3.43 ± 0.06	0.635	**0.674**	0.738	**0.038**
2 & 4	9	3.46 ± 0.05	0.802	**0.813**	0.821	**0.008**
2 & 3	9	1.73 ± 0.08	1.454	**1.471**	1.478	**0.011**

Table 4 TSC results using CONTOUR data (short separations)

Data	Runs	Separation interval, h	Minimum error, deg	Mean error, deg	Maximum error, deg	Standard deviation, deg
2 & 3	2	2.88 ± 0.03 hr	1.36	**1.38**	1.40	**0.03**
2, 3, 4	9	2.03 ± 0.17 hr	0.99	**1.24**	1.46	**0.14**
2, 3, 4	14	0.94 ± 0.08 hr	0.57	**1.11**	1.75	**0.34**
2, 3, 4	19	0.57 ± 0.08 hr	0.35	**1.24**	2.35	**0.58**

level. For the very short separation intervals of up to a few hours, the results are not very consistent and the attitude-determination error may vary considerably and reach values of 1 to 2 deg.

References

[1] van der Ha, J. C., "The Two-Sun Cones Attitude Determination Method," *Advances in the Astronautical Sciences*, Vol. 127, Pt. 1, 2007, pp. 117–130.

[2] van der Ha, J. C., Rogers, G., Dellinger, W., and Stratton, J., "CONTOUR Phasing Orbits: Attitude Determination & Control Concepts & Flight Results," *Advances in the Astronautical Sciences*, Vol. 114, No. 2, 2003, pp. 767–782.

[3] Reynolds, E., Panneton, P., Reinhart, M., Mehoke, D., Dellinger, W., Williams, S., Perschy, J., Harvey, R., and Carr, P., "Use of Hibernation Modes for Deep Space Missions as a Method to Lower Operations Cost," Utah State University, Logan, UT, Paper 01-8a-5, 13–16 Aug. 2001.

[4] van der Ha, J. C., and Lappas, V., "Autonomous Attitude Determination and Control of Low-Cost Deep Space Probe," *Proceedings of the 6th IAA International Conference on Low-Cost Planetary Missions*, ISAS/JAXA, Tokyo, Japan, 11–13 Oct. 2005, pp. 169–176.

[5] van der Ha, J. C., and Lappas, V., "Long-Term Attitude Drift of Spinning Spacecraft Under Solar Radiation Torques," *Journal of Guidance, Control, and Dynamics*, Vol. 30, No. 5, 2007, pp. 1470–1479.
doi:10.2514/1.28506

[6] Ottenstein, N. A., "Review of Spinning Spacecraft Dynamics Analyses and Inflight Experience," *Flight Mechanics Symposium*, NASA Goddard Space Flight Center, Greenbelt, MD, NASA TR 19990064192, May 1999.

[7] Vallado, D. A., *Fundamentals of Astrodynamics and Applications*, 2nd ed., Scientific and Business Media, New York, 2001, p. 183.

[8] Wertz, J. R. (ed.), *Spacecraft Attitude Determination and Control*, Scientific and Business Media, New York, 1978, Chap. 11.

[9] Shuster, M. D., "Efficient Algorithms for Spin-Axis Attitude Estimation," *Journal of the Astronautical Sciences*, Vol. 31, No. 2, April–June 1983, pp. 237–249.

[10] van der Ha, J. C., "Spin-Axis Attitude Determination Accuracy Model in the Presence of Biases," *Journal of Guidance, Control, and Dynamics*, Vol. 29, No. 4, July–Aug. 2006, pp. 799–809.
doi:10.2514/1.17745

[11] Gelb, A. (ed.), *Applied Optimal Estimation*, MIT Press, Cambridge, MA, 1974, p. 79.